Supporting Information

Soluble, Colorless and Biobased Polyimides with High Thermal Stability Derived from Renewable Anethole

*Fangyu Li[a], Yongzhen Wang[a], Jiawen Li[a], Haijiao Xie[b], Jiajia Wang[a,]**

[a]Key Laboratory of Polymeric Materials & Application Technology of Hunan Province, Key Laboratory of Advanced Organic Functional Materials of College of Hunan Province, College of Chemistry, Xiangtan University, Xiangtan 411105, Hunan Province, P. R. China

[b]Hangzhou Yanqu Information Technology Co., Ltd., Hangzhou 310003, P. R. China

Corresponding author e-mail: wangjiajia@xtu.edu.cn (Jiajia Wang)

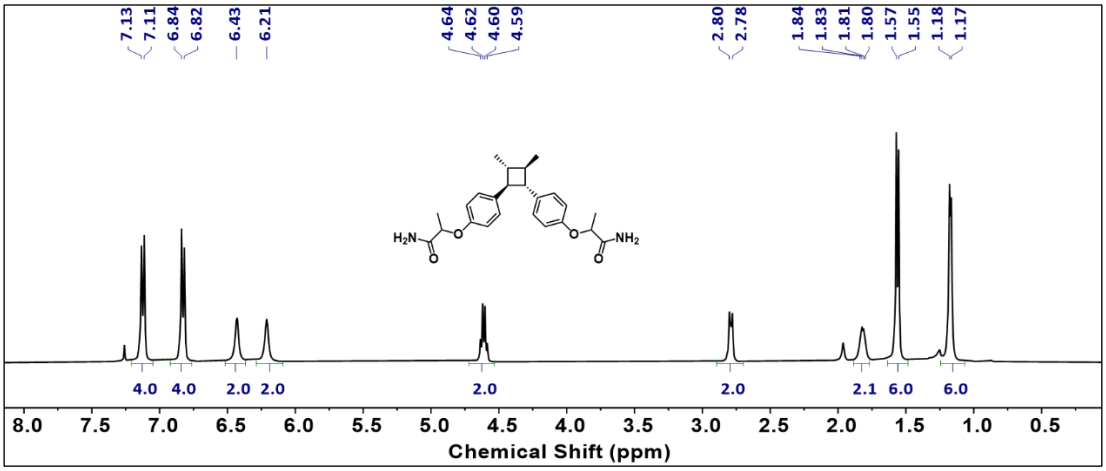

Fig. S1 ^{1}H NMR ($CDCl_3$, 400 MHz) of DAAM.

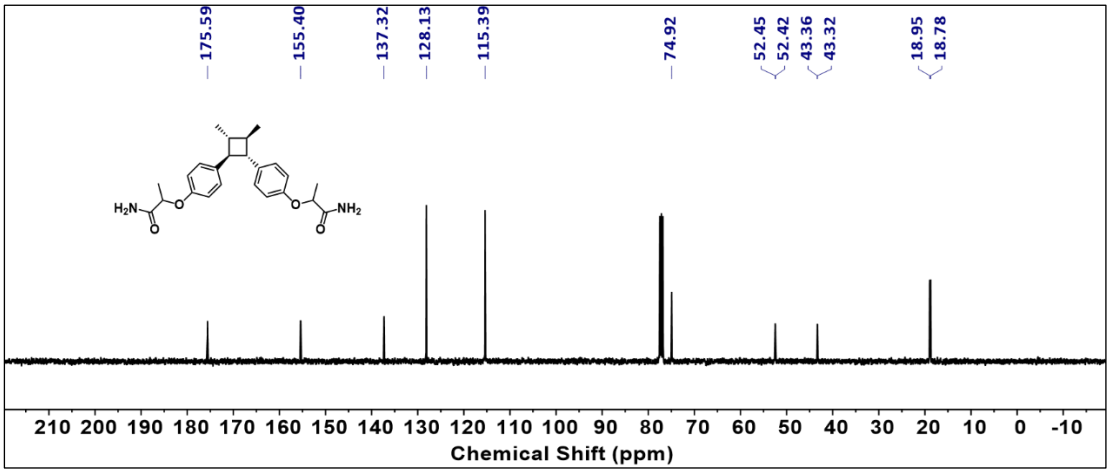

Fig. S2 ^{13}C NMR ($CDCl_3$, 100 MHz) of DAAM.

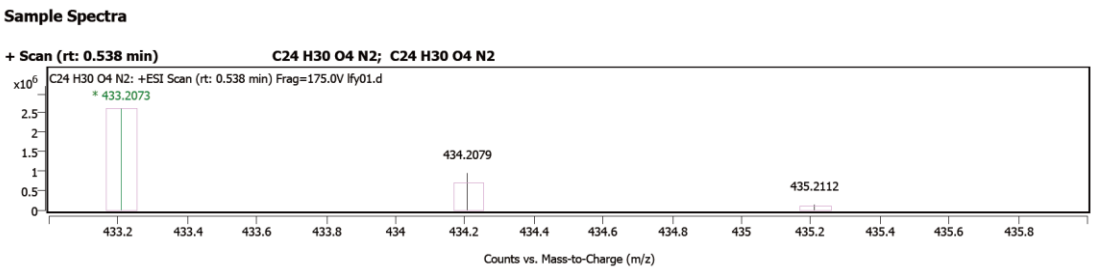

Fig. S3 HRMS spectrum of DAAM.

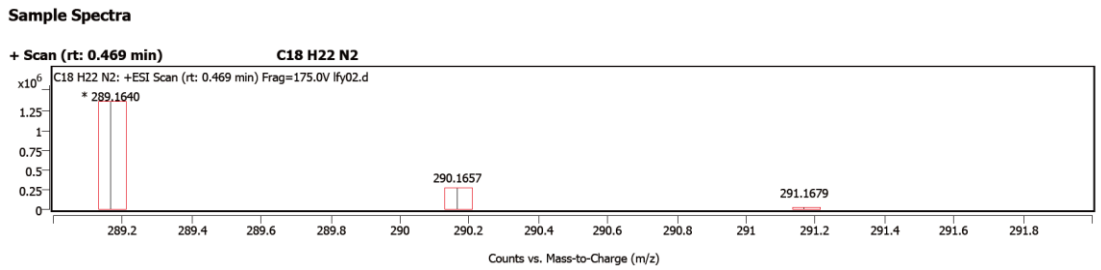

Fig. S4 HRMS spectrum of DAN.

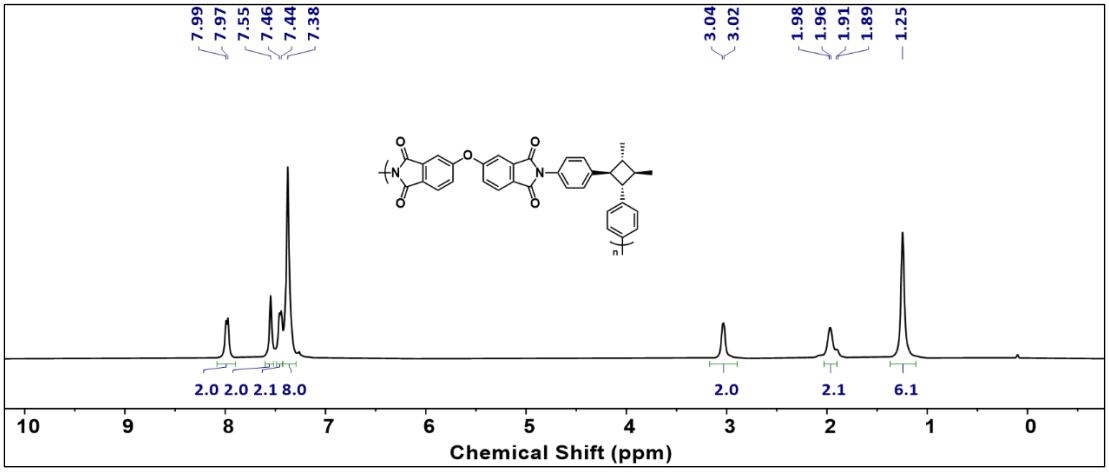

Fig. S5 ^{1}H NMR ($CDCl_3$, 400 MHz) of ODPA-DAN.

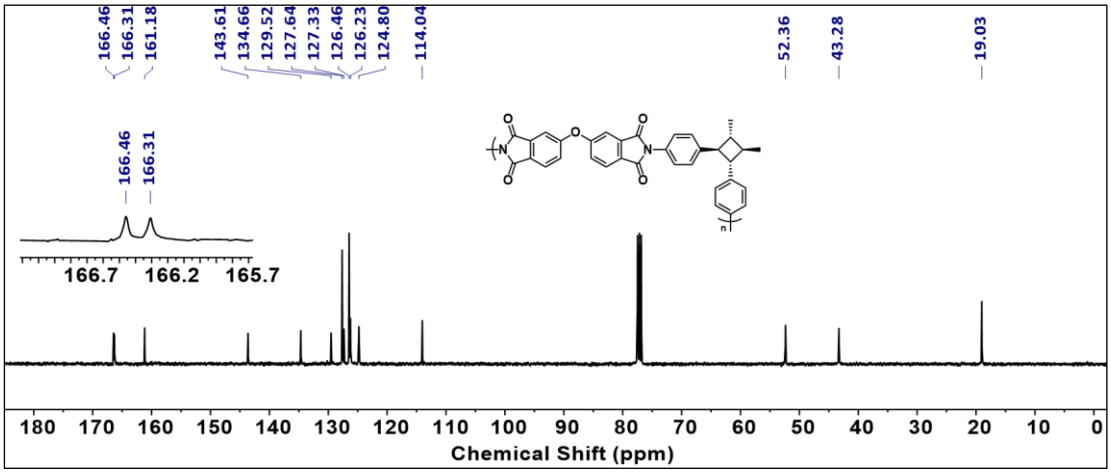

Fig. S6 ^{13}C NMR ($CDCl_3$, 100 MHz) of ODPA-DAN.

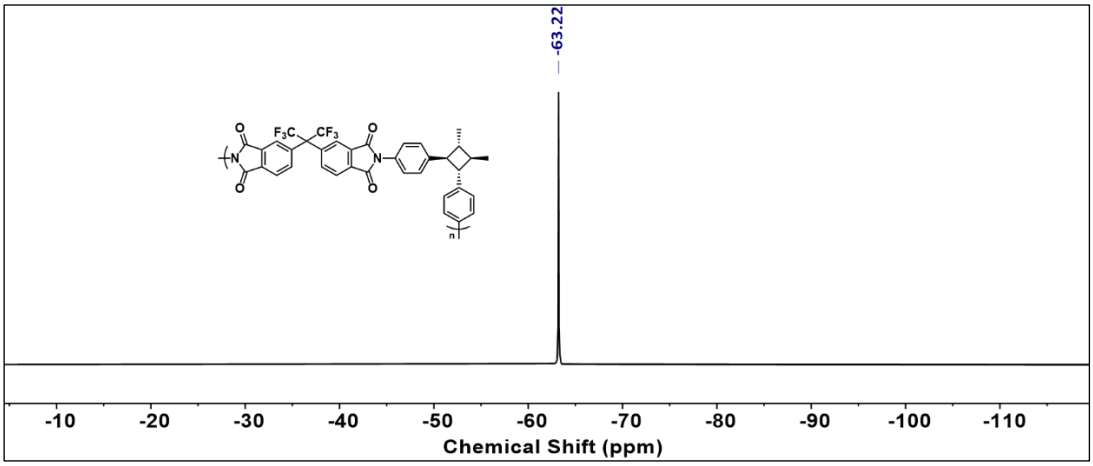

Fig. S7 ^{19}F NMR ($CDCl_3$, 376 MHz) of 6FDA-DAN.

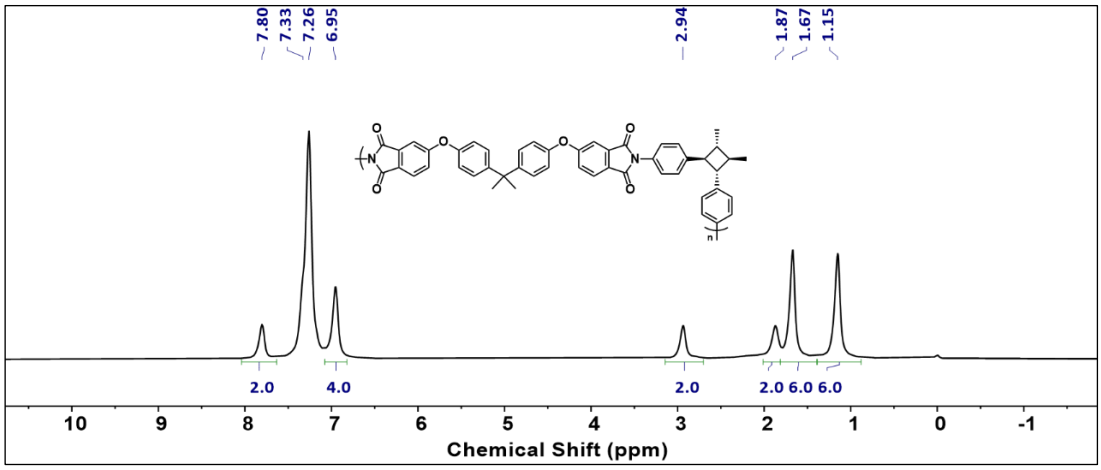

Fig. S8 ^{1}H NMR ($CDCl_3$, 400 MHz) of BPADA-DAN.

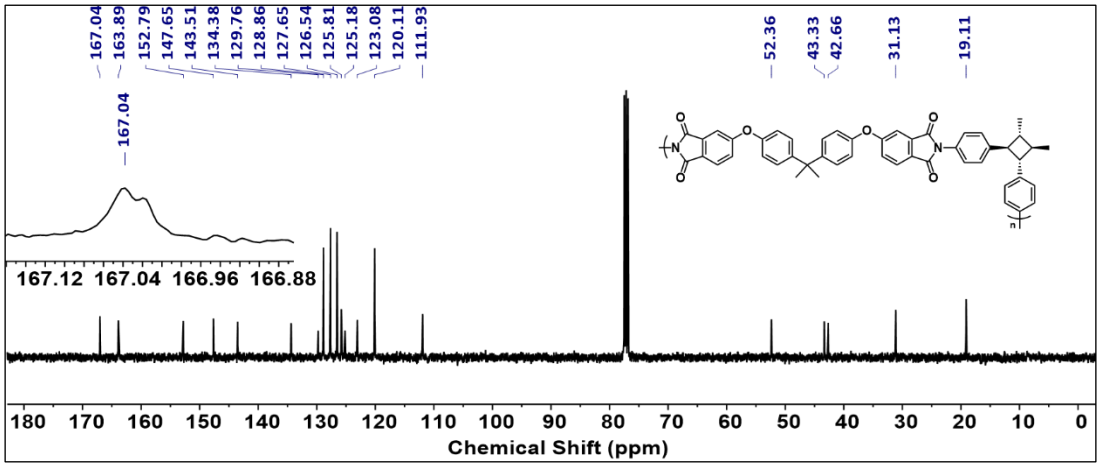

Fig. S9 ^{13}C NMR ($CDCl_3$, 100 MHz) of BPADA-DAN.

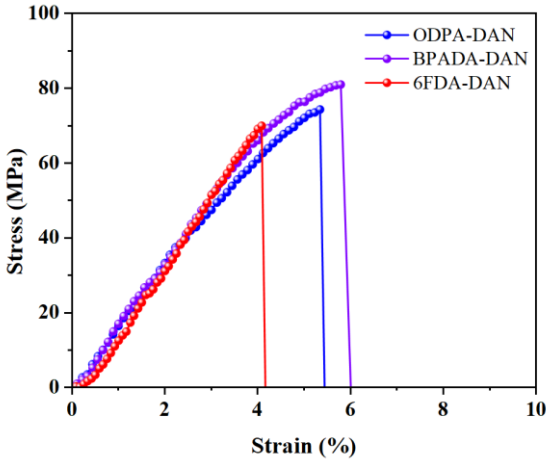

Fig. S10 Stress-strain curves of the biobased polyimides.

Table S1 Comparison of thermal properties and transparency between the biobased polyimides and other reported ones in literatures

Ref.	Name of monomer	Name of PI	T_g (°C)	T_{d5} (°C)	Transparency
This work	6FDA	6FDA-DAN	300	519	84% (450nm)
	ODPA	ODPA-DAN	265	470	82.7% (450nm)
1	OAC	PI(BAC)	302	328	2% (400nm)
		PI(FAC)	275	321	1.4% (400nm)
		PI(HAC)	219	291	83.5% (400nm)
	OOD	PI(BOD)	283	457	1% (400nm)
		PI(FOD)	288	456	1% (400nm)
		PI(HOD)	228	444	84.4% (400nm)
2	Daidzein-Based Dianhydride	PI-D-F	267.9	456.9	87% (450nm)
		PI-D-FO	280.4	487.7	84.1% (450nm)
		PI-D-O	302.6	517.8	78.5% (450nm)
	Daidzein-Based Dianhydride and Daidzein-Based Diamine	PI-D-D	318.2	550.6	75.90% (450nm)
	Daidzein-Based Diamine	PI-O-D	286.7	492.4	81.2% (450nm)
	ODPA	PI-O-O	258.5	446.5	86.8% (450nm)
3	αATA-Me	PI-1 (CBDA)	ND	365	88% (450nm)
	βATA-Me	PI-1 (CBDA)	ND	380	76% (450nm)
	αATA-Me	PI-2 (PMDA)	ND	410	80% (450nm)
	βATA-Me	PI-2 (PMDA)	ND	385	6% (450nm)
	αATA-Me	PI-3 (BTDA)	260	400	79% (450nm)
	βATA-Me	PI-3 (BTDA)	ND	385	52% (450nm)
	αATA-Me	PI-4 (ODPA)	250	400	69% (450nm)
	βATA-Me	PI-4 (ODPA)	230	395	73% (450nm)
	αATA-Me	PI-5 (DSDA)	275	410	
	βATA-Me	PI-5 (DSDA)	ND	380	
4	ISSDA	ISS-DACH	260	403	ND
		ISS-ADM	270	409	ND
		ISS-TFDB	258	400	ND
		ISS-TFMPD	265	409	ND
		ISS-PPD	268	409	ND
		ISS-MPD	260	403	ND
		ISS-ODA	240	409	ND
5	ISBA	PI(ISBA-BPDA)	257	418	
		PI(ISBA-CBDA)	276	408	80.2% (400nm)
		PI(ISBA-PMDA)	331	410	47.5% (400nm)
		PI(ISBA-BPDA)	257	418	70.1% (400nm)
		PI(ISBA-C95B5)	268	414	74.9% (400nm)

6	M1（H）	PI-1O	260	366	87% (450nm)
		PI-1F	281	368	83% (450nm)
	M2（CF3）	PI-2O	240	359	85% (450nm)
		PI-2F	279	363	87% (450nm)
7	MAAMB	API1	247	457	89.2% (500nm)
		API2	241	448	78.1% (500nm)
		API3	262	478	63.7% (500nm)
		API4	244	476	80.9% (500nm)
	1，4，4′-APB	SPI1	271	507	80.3% (500nm)
		SPI2	245	521	70.1% (500nm)
		SPI3	308	520	48.3% (500nm)
		SPI4	277	521	74.0% (500nm)
8	4ATA（-CH3）	PI-1m	ND	365	88.2% (450nm)
	4ATA（-CH2CH3）	PI-1e	ND	380	86.9% (450nm)
	4ATA（-CH3）	PI-2m	ND	410	80.1% (450nm)
	4ATA（-CH2CH3）	PI-2e	ND	380	50.7% (450nm)
	4ATA（-CH3）	PI-3m	260	400	79.1% (450nm)
	4ATA（-CH3）	PI-4m	250	400	68.9% (450nm)
	4ATA（-CH3）	PI-5m	240	395	65.4% (450nm)
	4ATA（-CH3）	PI-6m	275	410	82.2% (450nm)

Computational Details

All calculations were carried out with the Gaussian 16 software. The B3LYP functional was adopted for all calculations.[9] For geometry optimization and frequency calculations, the def2-SVP basis set[10] was used, and the optimal geometry for each compound was determined. The singlet point energy calculations were performed with a larger basis set def2-TZVP basis set. The DFT-D3 dispersion correction with BJ-damping[11,12] was applied to correct the weak interaction to improve the calculation accuracy. Orbital energy level analysis was performed by Multiwfn software.[13] The visualization of the orbitals for the repeating units were achieved using VMD software.[14]

References

1. X. Jiang, Y. Long, K. Chen, Q. Yu, L. Jiang, Z. Chi, S. Liu, J. Xu and Y. Zhang, *J. Mater. Chem. C*, 2023, **11**, 1082-1094.
2. C. Gong, Z. Liu, Z. Tao, A. Xu, H. Xie, Q. Fang, Z. Qiu and Y. Yan, *ACS Sustainable Chem. Eng.*, 2023, **11**, 4789-4799.
3. T. Noda, T. Iwasaki, K. Takada and T. Kaneko, *Macromolecules*, 2021, **54**, 10271-10278.
4. R. Sawada and S. Ando, *Macromolecules*, 2022, **55**, 6787-6800.
5. C.-K. Chen, Y.-C. Lin, L.-C. Hsu, J.-C. Ho, M. Ueda and W.-C. Chen, *ACS Sustainable Chem. Eng.*, 2021, **9**, 3278-3288.
6. R. Zhang, T. Li, H. Zhou, H. Huang and Y. Chen, *React. Funct. Polym.*, 2018, **128**, 91-96.
7. Z. Wang, Y. Li, T. Zhu, L. Xiong, F. Liu, H. Qi, *Polym. Degrad. Stabil.* 2019**, 167**, 67-76.
8. P. Suvannasara, S. Tateyama, A. Miyasato, K. Matsumura, T. Shimoda, T. Ito, Y. Yamagata, T. Fujita, N. Takaya and T. Kaneko, *Macromolecules*, 2014, **47**, 1586-1593.
9. A. D. Becke, *J. Chem. Phys.* **1993**, *98*, 5648-5652.
10. F. Weigend and R. Ahlrichs, *Phys. Chem. Chem. Phys.* **2005**, *7*, 3297.
11. S. Grimme, S. Ehrlich and L. Goerigk, *J. Comp. Chem.* **2011**, *32*, 1456-1465.
12. S.Grimme, J.Antony, S.Ehrlich and H.Krieg, *J. Chem. Phys.* **2010**, *132*, 154104/
13. Tian Lu, Feiwu Chen, *J. Comput. Chem.* **2012**, 33, 580-592.
14. Humphrey, W., Dalke, A. and Schulten, K. J. Molec. *Graphics* **1996**, *14*, 33-38.